Effect of crystallization and of water uptake on the free-volume hole size in polyamides 6 and 66

Effect of crystallization and of water uptake on the free-volume hole size in polyamides 6 and 66

G Dlubek†‡, M Stolp§, Ch Nagel§, H M Fretwell‖, M A Alam‡ and H-J Radusch§

† ITA Institut für innovative Technologien GmbH Köthen, Außnstelle Halle, Edvard-Grieg-Weg 8, D-06124 Halle/S, Germany
‡ University of Bristol, H H Wills Physics Laboratory, Tyndall Avenue, Bristol BS8 1TL, UK
§ Martin-Luther-Universität Halle-Wittenberg, Fachbereich Physik und Fachbereich Werkstof-fwissenschaften, D-06099 Halle/S, Germany
‖ Department of Physics, University of Illinois at Chicago, 845 W Taylor Street, Chicago, IL 60607-7059, USA

Abstract. Positron lifetime spectroscopy has been applied to estimate the free-volume hole sizes in the polyamides (nylons) 6 and 66 exposed to quenching, crystallization and water uptake. Three well separated peaks were observed in the lifetime distribution analysed via the MELT routine, the third of which (o-Ps) was found to split into two sub-peaks. From the analysis of computer generated spectra we were unable to conclude whether the sub-lifetimes represent two real annihilation channels or whether they appear as an artefact of analysing very broad o-Ps lifetime distributions. Assuming that the two lifetimes reflect the real situation $\tau_{3(i)} \sim 1.3$ ns may be attributed to o-Ps annihilation from crystallites and $\tau_{3(ii)} = 1.8$–2.2 ns from free-volume holes of the amorphous phase. Indications were found that during crystallization of quenched polyamides the hole size increases. Water uptake of the polyamides also leads to an increase in the hole size which is attributed to plasticization of the polyamides.

1. Introduction

Many of the application based macroscopic properties of polymers crucially depend on the microstructure of the sub-nanometre local free-volume holes that arise as a consequence of the irregular molecular packing in these materials. A unique emerging tool to probe such holes is positron/positronium annihilation spectroscopy. In molecular materials, such as polymers, a significant fraction of the injected positrons annihilates from the positronium (Ps) [1] bound state. In matter, the relatively long-lived ortho-positronium (o-Ps: parallel electron and positron spins) undergoes numerous collisions with molecules during which the positron of the Ps may annihilate with an electron other than its bound partner and of opposite spin (pick-off annihilation). The result is a sharply reduced o-Ps lifetime depending on the frequency of collisions. In amorphous polymers, the positronium is preferentially formed and annihilated within these 'holes'. In this case, the collision frequency of the positronium with the surrounding medium will depend on the dimensions of the confining volume. This results in a highly sensitive correspondence of the o-Ps pick-off rate and therefore the lifetime to the hole size [2, 3].

In semicrystalline polymers Ps is expected to exist in and annihilate from both the densely packed crystalline phase (possibly in the 'interstitial' spaces between the 'crystalline planes') and the holes in the amorphous phase [4]. This may lead to two distinct sets of o-Ps pick-off lifetimes (or lifetime distributions). Two sets of lifetime distributions have indeed been observed in a number of semicrystalline polymers. In polymers such as PTFE or PE the two lifetime distributions are well separated in the time scale and can be resolved in an experiment and subsequent data analysis with sufficient confidence. In cases where the two distributions lie in close proximity to each other, their extraction in the analysis is less straightforward. One of the goals of this paper is to address the issue of the existence of two ortho-positronium states and their possible physical relevance in two polyamide polymers (PA6 and PA66) in amorphous (quenched) and partially crystalline (annealed) forms. Here, the two possible lifetime distributions lie close enough to each other and standard data analyses provide ambiguous results. To attempt to overcome this, we measured lifetime spectra with extreme high statistical accuracy ($\sim$50 million counts in each spectrum). In addition, we tested the reliability of our analysis procedure through the analysis of computer generated spectra and comparing the results with the analysis of our experimental data. A second goal of this paper has been to study the effect of crystallization and water uptake on the local free volumes in PA6 and PA66.

2. Experiment and data analysis

The PA6 and PA66 specimens under investigation were commercial polymers supplied by BASF, Germany. Thin slices (0.1 mm) of the material were quenched from 250 °C into ethanol at −70 °C. Following the quench, the PA6 and PA66 specimens were subjected to: (1) an anneal at 60 °C for 1 hour; (2) an anneal at 200 °C for 1 hour; (3) immersion into water at room temperature for a period of 6 days; (4) immersion into boiling water for 18 hours. During the treatment (3) and (4), the water uptake was estimated via a measurement of the sample weight. The crystallinities of the quenched and annealed samples were probed by wide angle x-ray spectroscopy (WAXS) [5]. Positron lifetime measurements [1] with a high total count of 5×10^7 were carried out using a conventional fast–fast coincidence system with a time resolution of $\sim$260 ps (FWHM).

For a detailed analysis of the lifetime spectra $s(t)$, we used the program MELT (maximum entropy for lifetime analysis [6]) which assumes a continuous lifetime distribution. These were complemented by the Laplace inversion technique using the routine CONTIN [13] which also returns a continuous distribution of lifetimes. In addition, we applied the conventional analysis in terms of a weighted sum of discrete exponentials, $s(t) = \sum (I_i/\tau_i) \exp(-t/\tau_i)$ [1], using the routine LIFSPECFIT (developed by the positron group of the Helsinki University of Technology, version 5.1, 1992, unpublished). τ_i denotes the mean (characteristic) lifetime of the positron/Ps state i, while I_i is the intensity of the corresponding lifetime component. The parameters are obtained from a non-linear least-squares fitting of $s(t)$ to the experimental spectra [1]. Instead of discrete components (δ-functions), the routines MELT and CONTIN deliver a lifetime distribution consisting of Gaussian-like peaks. The characteristic lifetime τ_i of the peak i and its intensity I_i are calculated as the mass centre and relative area of the corresponding peak. Others than in MELT and CONTIN, the number of fitted exponentials has to be assumed using the routine LIFSPECFIT.

3. Results and discussion

In the discrete exponential terms analysis of the lifetime spectra, fits with a variance of 1.8–2.5 and 1.1–1.3 could be achieved by assuming three and four lifetime components. In the four component analysis, two components are returned in the nanosecond range. Three well separated main peaks appear in the polyamide lifetime distributions when analysed by the MELT routine. The longest lived component splits into two sub-peaks for low entropy weights (figure 1). The lifetimes correspond to annihilation of p-Ps ($\tau_1 = 158$–182 ps), free positrons ($\tau_2 = 360$–390 ps) and o-Ps pick-off ($\tau_{3(i)} \sim 1.3$ ns and $\tau_{3(ii)} = 1.8$–2.2 ns). The corresponding intensities varied in the ranges: I_1 between 20 and 24%, I_2 between 55 and 59%, $I_{3(i)} \sim 13\%$, $I_{3(ii)} \sim 12\%$. In the existing literature, the polyamides are reported to have only three component positron lifetimes [7, 9]. Although the lifetime distributions obtained from the Laplace inversion technique are similar to the solutions given by the maximum entropy analysis, the separation of the o-Ps sub-lifetimes is much clearer in the latter case. In the following, we discuss the three- and four-component analysis of the spectra and their consequences on the interpretation of the physical picture separately.
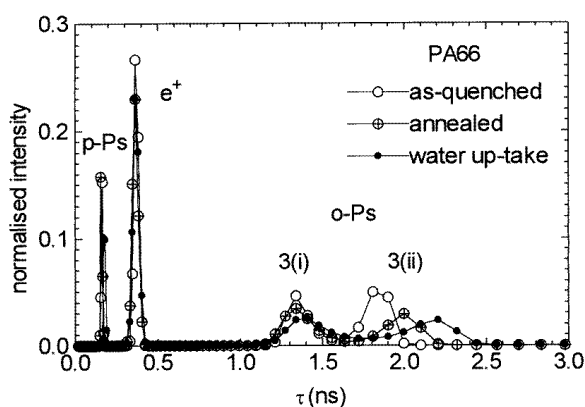

Figure 1. Positron lifetime intensity distribution in as-quenched (empty circles), annealed (200 °C, 1 h, cross-centred circles) and water immersed (100 °C, 18 h, filled circles) PA66. The distributions were obtained by using the lifetime analysis routine MELT, entropy weight $E = 5 \times 10^{-8}$.

3.1. Three-component analysis of positron lifetimes

The lifetimes obtained from a three-discrete-exponential fit (LIFSPECFIT) we denote by τ_1^*, τ_2^* and τ_3^*. The o-Ps lifetime τ_3^* and its relative intensity I_3^* are shown in figure 2. Following the quench, τ_3^* has a value of 1620 ps in both polyamides which agrees with previous measurements by others [7–9]. This lifetime is attributed to the o-Ps pick-off annihilations from free volume holes in the amorphous phase. Its size may be estimated via

$$\tau_{po} = 0.5 \text{ ns} \left[1 - \frac{r}{r + \delta r} + \frac{1}{2\pi} \sin\left(\frac{2\pi r}{r + \delta r}\right) \right]^{-1}. \tag{1}$$

Here τ_{po} denotes the lifetime due to Ps pick-off annihilation which may be identified with $\tau_{3(ii)}$ or τ_3^* and $\delta r = 0.166$ nm [2, 3].

The o-Ps lifetimes τ_3^* in the as-quenched polyamides correspond to a hole size of $r = 0.248 \pm 0.003$ nm and $v = 4\pi r^3/3 = 0.064 \pm 0.003$ nm^3 (equation (1)). During
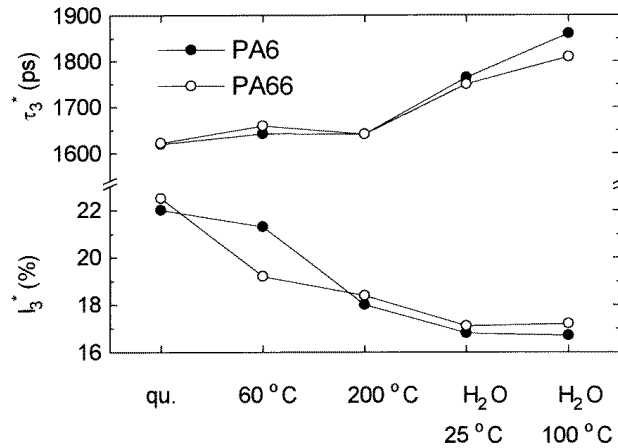
Figure 2. Changes of the lifetime τ_3^* and the intensity I_3^*, obtained from a three-component fit of the lifetime spectra (using LIFSPECFIT), in PA6 and PA66 due to different sample treatments. The statistical errors correspond to the size of data points.

annealing at 60 °C and 200 °C, τ_3^* remains largely constant, but its intensity I_3^* decreases in PA66 from 22.5% (in the as-quenched state) through a value of 19.2% to 17.5% (figure 2). Only a slight decrease of I_3^* is observed during annealing of PA6 at 60 °C, but it reaches a value similar to that of PA66 after an anneal at 200 °C. From our WAXS investigations we estimated the following degrees of crystallinity for the variously treated specimens: PA6: ∼2% (60 °C) and 18% (200 °C); PA66: 15% (60 °C) and 28% (200 °C, also refer to [5]). The as-quenched samples were considered to be predominantly amorphous. These results would suggest that the strong (weak) crystallization of PA66 (PA6) after an anneal at 60 °C may be responsible for the strong (weak) decrease in the o-Ps intensity I_3^*. Treatments of the samples in water environments at various temperatures leads to an increase in τ_3^* from 1620 ps to ∼1750 ps (25 °C, 6 days, 4.5 wt% water uptake) and finally to ∼1850 ps (100 °C, 18 hours, 9 wt% water uptake) while the intensity I_3^* exhibits only a small decrease. Similar effects were found previously [7–9]. From τ_3^* and equation (1) it is estimated that the hole size increases from $r = 0.248$ nm before the water uptake to a maximum value of 0.271 nm ($v = 0.083$ nm^3). The polyamides are 'cross linked' by hydrogen bonds between the NH and CO groups. In the presence of water within the sample, some of the hydrogen bonds are broken up and replaced by water molecules. This leads to an increase in the mobility of the polymer chains and a consequent decrease in the glass transition temperature T_g [10, 11]. Such plasticization effects are compatible with the observed increase in the free-volume hole size with increasing water uptake.

3.2. Four-component analysis of positron lifetimes

As mentioned earlier, low regularization of the MELT solutions (i.e. an entropy weight of $E = 5 \times 10^{-8}$ which provides the 'optimum solution' following the criteria given by Shukla *et al* [6]) of our high statistics lifetime spectra (∼50 million counts per spectrum), or a four-discrete-term LIFSPECFIT analysis, leads to the appearance of two o-Ps peaks in the lifetime distribution. The lower o-Ps peak has its mass centre at $\tau_{3(i)} = 1340$ ps for quenched or annealed PA66 and at 1460 ps for water immersed PA66. The longer

o-Ps lifetime increases with the treatment from $\tau_{3(ii)} = 1820$ ps (quenched) via 1940 ps (annealed) to 2140 ps (water immersed PA66, see figure 1).

The existence of two o-Ps lifetimes would be in line with similar observations in other semicrystalline polymers where these two lifetimes are well separated [4]. In the present case, due to the close proximity of the two o-Ps lifetimes and the limited resolving power of the lifetime technique (see [12] for a detailed discussion), neither the validity of the existence of these o-Ps sub-lifetimes nor their interpretation is straightforward. Limitations in the analysis may result in erroneously assigned peak positions (in time scale) and the intensities of the various components due to a variety of factors. To assess the possible sources of errors in the analysis of the experimental data in terms of four components, we performed computer simulation tests. Synthetic lifetime spectra with parameters close to the observed ones in polyamides were generated.

First, we simulated lifetime spectra with discrete components. τ_1 and τ_2 and their intensity values are taken from our experimental analysis to which two discrete neighbouring o-Ps components, each of 12.5% intensities, are added. The lifetime $\tau_{3(ii)sim}$ was fixed to 2.0 ns, while $\tau_{3(i)sim}$ was varied between 1.0 and 2.0 ns. After adding a contribution arising from the positron source, these spectra were convoluted with the experimental resolution function (assumed to be Gaussian). Finally, a background and appropriate Poisson noise were added to each channel. Ten spectra were generated for each parameter set in order to estimate the statistical error in the data analysis. As shown in figure 3, the analysed lifetimes (symbols) agree well with the simulation inputs (solid lines) in the range below $\tau_{3(i)sim} = 1.3$ ns. Above this value of $\tau_{3(i)sim}$, the analysed $\tau_{3(ii)}$ diverges from the input of 2 ns and approaches the weighted average value of both components (dotted line). At the same time, $\tau_{3(i)}$ also shows a significant decrease (from its input value) together with a dramatic increase in the statistical error. An analogous behaviour is observed in $I_{3(i)}$ (not shown). Above $\tau_{3(i)sim} \approx 1.5$ ns, the analysis procedures are unable to resolve both o-Ps components and a single component with an 'apparent' lifetime and intensity of $\tau_{3,app} = (I_{3(i)}\tau_{3(i)} + I_{3(ii)}\tau_{3(ii)})/(I_{3(i)} + I_{3(ii)})$ and $I_{3,app} = I_{3(i)} + I_{3(ii)}$ is observed.
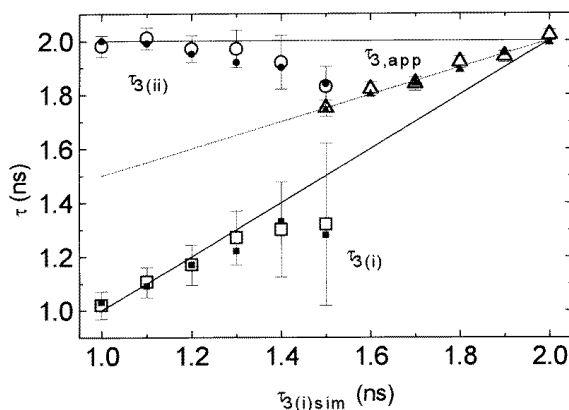

Figure 3. Plot of the o-Ps lifetimes $\tau_{3(i)}$ and $\tau_{3(ii)}$ obtained via the MELT (filled symbols) and CONTIN (empty symbols) analysis of simulated lifetime spectra (50 M total counts) as a function of the lifetime $\tau_{3(i)}$ assumed in simulations. Other parameters have been fixed in simulations to: $\tau_1/I_1 = 150$ ps/18%; $\tau_2/I_2 = 360$ ps/57%; $I_{3(i)} = 12.5\%$; and $\tau_{3(i)}/I_{3(ii)} = 2000$ ps/12.5%. The straight lines indicate the simulated lifetimes $\tau_{3(i)}$ and $\tau_{3(ii)}$ while the dash–dotted line represents the average of the simulated $\tau_{3(i)}$ and $\tau_{3(ii)}$.

From these simulations using discrete components, we may conclude that the double peak structure in the o-Ps lifetime distribution (figure 1) may be due to two close but 'discrete' (or of narrow distribution) lifetimes situated in the range $\tau_{3(i)} = 1.3$–1.5 ns and $\tau_{3(ii)} \approx 2$ ns for as-quenched PA66, for example. The higher the value of $\tau_{3(ii)}$ the more accurate is the discrete analysis of both lifetimes.

In figure 4, we present the results of the analysis of simulated spectra containing the same discrete τ_1, τ_2 and their intensities as above and a single and broad Gaussian distribution for τ_3. The aim is to illustrate the effect of distributed o-Ps lifetimes on the analysed lifetime parameters. In the simulation of the o-Ps lifetime distribution, we assumed a Gaussian with the centre at $\tau_{3,sim} = 1.8$ ns, an intensity of $I_{3,sim} = 25\%$ and a standard deviation of $\sigma_{3,sim}$ which was varied between 0 and 800 ps. We observe that the ability to resolve a finite width of the distributions by the programs starts at $\sigma_{3,sim} \approx 60$ ps for MELT but only at ~150 ps for CONTIN. The width of the o-Ps lifetime distribution analysed with both routines broadens with increasing $\sigma_{3,sim}$. At $\sigma_{3,sim} \approx 400$ ps, however, both routines tend to split the broad o-Ps lifetime distribution into two sub-peaks. Their mass centres appear approximately at the lifetimes $\tau_{3(i)app} = 1.8$ ns $- \sigma_{3,sim}$ and $\tau_{3(ii)app} = 1.8$ ns $+ \sigma_{3,sim}$. Their intensities behave like $I_{3(i)app} \approx I_{3(ii)app} \approx I_{3,sim}/2$.
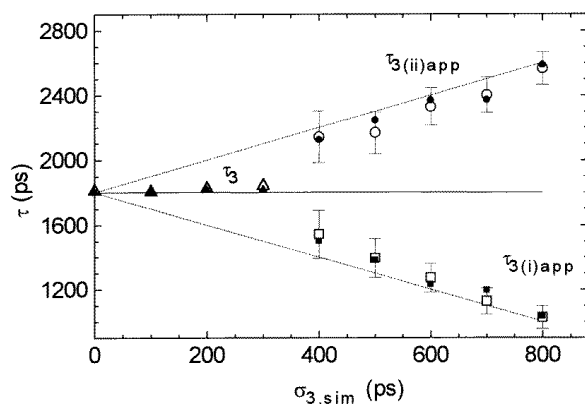

Figure 4. As in figure 3, but in the simulations a single o-Ps component with a lifetime of $\tau_3 = 1800$ ps, an intensity of $I_3 = 25\%$ and a Gaussian distribution of a standard deviation σ_3 between 0 and 800 ps were assumed. The analysed lifetimes are plotted as function of σ_3 assumed in simulations.

The conclusion from this simulation is that for larger widths of the o-Ps lifetime distributions both routines MELT and CONTIN are unable to analyse these distributions correctly but deliver as an artefact two neighbouring sub-lifetimes. Unfortunately, this artefact cannot be distinguished from a real occurrence of two (discrete) neighbouring lifetimes. The results of the simulation show that it is not clear how to interpret the lifetime distributions shown in figure 1. Nevertheless, in light of the observation of two clearly distinguishable o-Ps lifetimes in other semi-crystalline polymers such as PE and PTFE [4], the observation in figure 1 cannot be arbitrarily ignored. Assuming that the sub-peaks represent different o-Ps annihilation channels we may attribute the medium lifetime, $\tau_{3(i)} \approx 1.3$ ns, to o-Ps annihilation from crystalline regions in the polyamides [4] and the longer lifetime, $\tau_{3(ii)} = 1.8$–2.2 ns, to annihilations of o-Ps from holes in the amorphous phase. On this basis, below, we present a possible physical scenario to explain our observations as a function of sample treatment.

The o-Ps lifetime $\tau_{3(ii)} = 1820$ ps observed in quenched PA66 corresponds to a hole size of $r = 0.271$ nm and $v = 0.083$ nm^3 (equation (1)). As a consequence of crystallization $\tau_{3(ii)}$ increases to 1940 ps (figure 1). If this increase is a real effect (rather than an artefact of data analysis), it reflects an increase in the hole size to $r = 0.280$ nm and $v = 0.092$ nm^3. This behaviour is not unphysical and may be explained in the following terms. After rapid quenching, the sample is in an almost complete amorphous state. During the annealing of the quenched specimen, crystallites grow and finally occupy a volume fraction which, according to relative x-ray intensity, is of the order of 17 to 28%. The crystallites have a higher density than the amorphous phase. The higher density of the crystallites corresponds to a lower specific volume. The decrease in the specific volume in local regions during the anneal is likely to cause a tension stress acting on the surrounding amorphous phase. This tension stress may lead to an increase in the free-volume hole size within the amorphous regions which may then be observed as an increase of the o-Ps lifetime. From the increase in the hole volume we may speculate that the density of the amorphous phase decreases during crystallization and probably also as a function of crystallinity X_c. This conclusion would have important practical consequences in the estimation of the degree of crystallinity from the relative value of the density ρ of semicrystalline polymers. In such an estimation it is assumed that densities of the crystalline and the amorphous phases do not change as function of X_c [14].

Unfortunately, there is no way to estimate the absolute number of holes appearing in the amorphous phase from positron experiments alone. An approximate estimate can be arrived at by relating the hole size observed by the Ps to differences in the densities of the amorphous and crystalline phases. We assume that the total (specific) volume of an amorphous polymer may be subdivided into the volume formed by the holes, V_h, and a hypothetical volume which we call bulk volume V_b, $V_a = V_h + V_b$. In semicrystalline polymers, the specific bulk volume may be approximated by the specific volume of the crystalline phase, V_c. It represents the most dense packing of a given polymer and is composed of the actually occupied volume–the van der Waals volume—and a free volume which may be called interstitial free volume. The interstitial free volume is the supplement of the crystalline packing density to 100%.

From this we obtain for the fractional free or hole volume [4]

$$h = (V_a - V_c)/V_a = 1 - V_c/V_a = 1 - \rho_a/\rho_c \qquad (2)$$

where $V_a = 1/\rho_a$ and $V_c = 1/\rho_c$ denote the specific volume and ρ_a and ρ_c the density of the polymer in the amorphous (either glassy or rubbery) phase and in the crystalline phase. With $\rho_a = 1.08$ g cm^{-3}, $\rho_c = 1.23$ g cm^{-3} for PA6 and $\rho_a = 1.07$ g cm^{-3}, $\rho_c = 1.24$ g cm^{-3} for PA66 we obtain $h = 0.123$ (PA6) and 0.138 (PA66). The number of holes we may now estimate from $N = h/v_a$. With $v_a \approx 0.09$ nm^3 we estimated $N \approx 1.4 \times 10^{27}$ m$^{-3} = 1.4$ nm^{-3}. This value is in good correspondence to previous estimates for polyethylene (0.73 nm^{-3} [4]), Teflon (0.36 nm^{-3} [4]) and poly(diethylene glycol bis(allyl carbonate) networks (0.8–1.3 nm^{-3} [15]) which were obtained from the comparison of hole volume and macroscopic volume thermal expansion [4].

By immersing the PA66 sample in boiling water, the o-Ps lifetime was found to increase to $\tau_{3(ii)} = 2140$ ps. This value corresponds to a hole size of $r = 0.298$ nm and $v = 0.111$ nm^3 which is distinctly larger than estimated from τ_3^* ($r = 0.248$ nm, $v = 0.083$ nm^3). This result shows the importance of the need to be able to separate all possible o-Ps lifetime components in a given spectrum. In this context we note that, when τ_3^* is due to an average over two or more o-Ps lifetimes, it may change when either

the individual lifetimes and/or their intensities change. Therefore, the observed values and variations in τ_3^* may be wrongly interpreted.

In the light of the simulation studies, the behaviour observed in figure 1 may also arise from a single but broad o-Ps lifetime distribution. In that case, the centre of the distributions are found at $[\tau_{3(i)}I_{3(i)} + \tau_{3(ii)}I_{3(ii)}]/(I_{3(i)} + I_{3(ii)}) \approx \tau_3^*$, their standard deviation may be estimated via $\sigma_3^* \approx (\tau_{3(ii)} - \tau_{3(i)})/2$. Figure 1 would then indicate that the centre of the hole size distribution and its width increases due to crystallization and water uptake by the polyamides. This conclusion is also not unphysical. The range of the hole size distributions (FWHM) may be estimated from our data to be $r = 0.210\text{--}0.272$ nm ($v = 0.039\text{--}0.084$ nm^3, quenched samples), $r = 0.209\text{--}0.284$ nm ($v = 0.038\text{--}0.096$ nm^3, crystallized samples) and $r = 0.224\text{--}0.302$ nm ($v = 0.047\text{--}0.117$ nm^3, following water uptake).

Acknowledgments

References

[1] Mogensen O E 1995 *Positron Annihilation in Chemistry* (Heidelberg: Springer)
[2] Eldrup M, Lightbody D and Sherwood J N 1981 *Chem. Phys.* **63** 51
[3] Nakanishi H and Jean Y C 1988 *Positron and Positronium Chemistry, Studies in Physical and Theoretical Chemistry* vol 57, ed D M Schrader and Y C Jean (Amsterdam: Elsevier) p 159
[4] Dlubek G, Saarinen K and Fretwell H M 1998 *J. Polym. Sci.* B **36** 1513
[5] Androsch R, Stolp M and Radusch H-J 1996 *Acta Polym.* **47** 104
[6] Shukla A, Peter M and Hoffmann L 1993 *Nucl. Instrum. Methods* A **335** 310
[7] Chuang S Y, Tao J and Wilkenfeld J M J 1972 *Appl. Phys.* **43** 737
[8] Singh J J, Clair T L St, Holt W H and Mock W Jr 1984 *Nucl. Instrum. Methods* **221** 427
[9] Welander M and Maurer F H 1992 *J. Mater. Sci. Forum* **105–110** 1815
[10] Oark Y, Ko J, Ahn T-K and Choe S 1997 *J. Polym. Sci.* B **35** 807
[11] Deopura B L, Sengupta A K and Verma A 1983 *Polym. Commun.* **24** 287
[12] Dlubek G, Hübner Ch and Eichler St 1998 *Nucl. Instrum. Methods* B **142** 191
[13] Gregory R B and Zhu Y 1990 *Nucl. Instrum. Methods* A **290** 172
[14] Billmeyer F W Jr 1984 *Textbook of Polymer Science* (New York: Wiley) p 288
[15] Dlubek G, Stejny J and Alam M A 1998 *Macromolecules* **37** 4574